

# 1 Transferrin Receptor Targeting Chimeras (TransTACs) for Membrane Protein Degradation

## 2 Authors & Affiliations:

3 Dingpeng Zhang<sup>1,2</sup>, Jhoely Duque-Jimenez<sup>1</sup>, Garyk Brixi<sup>3</sup>, Francesco Facchinetti<sup>4-6</sup>, Kaitlin Rhee<sup>1,2</sup>, William W.  
4 Feng<sup>4-6</sup>, Pasi A. Jänne<sup>4-7</sup>, Xin Zhou<sup>1,2\*</sup>  
5

6  
7 <sup>1</sup>Department of Cancer Biology, Dana-Farber Cancer Institute, Boston, MA, USA

8 <sup>2</sup>Department of Biological Chemistry and Molecular Pharmacology, Harvard Medical School, Boston, MA,  
9 USA

10 <sup>3</sup>Harvard University, Boston, MA, USA

11 <sup>4</sup>Department of Medical Oncology, Dana-Farber Cancer Institute, Boston, MA, USA

12 <sup>5</sup>Department of Medicine, Harvard Medical School, Boston, MA, USA

13 <sup>6</sup>Lowe Center for Thoracic Oncology, Dana-Farber Cancer Institute, Boston, MA, USA

14 <sup>7</sup>Belfer Center for Applied Cancer Science, Dana-Farber Cancer Institute, Boston, MA, USA

15 \*Corresponding Author: [xin\\_zhou1@dfci.harvard.edu](mailto:xin_zhou1@dfci.harvard.edu)

## 16 17 Abstract

18 Cancer cells require high levels of iron for rapid proliferation, leading to a significant upregulation of the  
19 iron carrier protein Transferrin Receptor (TfR) on their cell surface. Leveraging this phenomenon and the  
20 exceptionally fast endocytosis rate of TfR, we introduce Transferrin Receptor TArgeting Chimeras (TransTAC),  
21 a novel molecular archetype for membrane protein degradation in cancers and other cell types. TransTACs  
22 repurpose the naturally recycling receptor TfR1 for protein degradation. To accomplish this, we utilized a  
23 combination of protein engineering strategies to redirect the target protein from recycling-endosome trafficking  
24 to lysosomal degradation. We show that TransTACs can highly efficiently degrade a diverse range of single-pass,  
25 multi-pass, native, or synthetic membrane proteins, establishing new possibilities for targeted cancer therapy.

## 26 27 Introduction

28 Targeted protein degradation (TPD) is a rapidly growing field in drug discovery and pharmacology.  
29 Complementing traditional drug modalities, TPD molecules offer a novel therapeutic mechanism to tackle  
30 challenging targets or increase the therapeutic potential of currently used drugs<sup>1</sup>. While most efforts in this field  
31 have focused on small molecules for intracellular targets, inducing targeted degradation of membrane proteins  
32 has recently emerged as a new therapeutic opportunity<sup>2</sup>. Membrane proteins are central to a myriad of cellular  
33 functions and serve as targets for over half of all drugs<sup>3</sup>. Therefore, developing universal strategies to degrade  
34 membrane proteins is of exceptional interest for both basic research and therapeutic intervention purposes.

35 Over the last few years, several proof-of-concept strategies for membrane receptor degradation have been  
36 described. These strategies use heterobifunctional biologics that recruit a specific “effector” protein such as a  
37 membrane E3 ligase<sup>4,5</sup> or a lysosome shuttling receptor<sup>6-8</sup> to the protein of interest (POI) to induce lysosome-  
38 mediated protein degradation. However, the effectiveness of these biological effectors is often limited by their  
39 tissue-specific expression patterns. GalNAc-LYTAC, for instance, targets the hepatocyte-specific receptor  
40 asialoglycoprotein receptor (ASGPR), making it only suitable for treating liver disease or clearing circulating  
41 targets<sup>6,9</sup>, while RNF43- or ZNRF3-based methods are more effective for treating Wnt-signaling upregulated

42 disorders where RNF43 and ZNRF3 are expressed at high levels<sup>4,5</sup>. Current technologies are therefore not able to  
43 cover the full spectrum of diseases, and developing alternative effectors overexpressed in different diseases and  
44 tissues would greatly expand the range of cell surface targets that can be regulated and also increase the targeting  
45 specificity.

46 Iron is an essential element for cells, and its transportation is facilitated by the transferrin receptor 1  
47 (TfR1)<sup>10,11</sup>. Rapidly dividing cells, such as cancer cells and activated immune cells, exhibit substantially increased  
48 TfR1 expression compared to non- or slow-dividing cells due to their high demand for iron<sup>12,13</sup>. As a result, TfR1  
49 is an attractive target for modulating these cell types. Several studies have investigated TfR1 as a therapeutic  
50 target for cancer with promising outcomes<sup>12,14</sup>, as well as for tumor imaging<sup>15</sup> and targeted drug delivery<sup>16</sup>.

51 Apart from its overexpression in proliferating cells, the rapid internalization rate is another intriguing  
52 feature of TfR1. As a classical recycling receptor, extensive research has been conducted on the intracellular  
53 trafficking pathways and internalization kinetics of TfR1. TfR1 exhibits an average internalization rate of 500  
54 molecules per cell per second, making it one of the fastest internalizing receptors known<sup>17,18</sup>. This exceptional  
55 speed suggests that TfR1 has the potential to serve as a carrier "effector" for inducing targeted internalization of  
56 membrane proteins.

57 In this study, we leveraged these two crucial features of TfR1 and employed protein engineering strategies  
58 to develop a novel technology for degrading membrane proteins. We call this technology Transferrin Receptor  
59 TArgeting Chimeras (TransTAC). TransTACs are heterobispecific antibodies that bring the POI and TfR in close  
60 proximity at the cell surface and separate them in the endosomes for lysosome-mediated degradation (**Fig. 1a**).  
61 We show that TransTACs are highly effective in degrading various types of membrane proteins, including single-  
62 pass, multi-pass, native, and synthetic receptors, showing a degradation efficiency of over 80% in various cellular  
63 systems. An intriguing characteristic of TransTACs is the fast kinetics of targeted internalization, which occurred  
64 on the timescale of minutes in the context of a chimeric antigen receptor (CAR). Moreover, TransTAC molecules  
65 are fully recombinant, versatile, and modular. These unique properties make TransTACs a promising tool for the  
66 precise manipulation of cell surface targets, particularly in cancer and immune cells, offering new opportunities  
67 for precise targeting of the extracellular proteome in research and medicine.

## 68

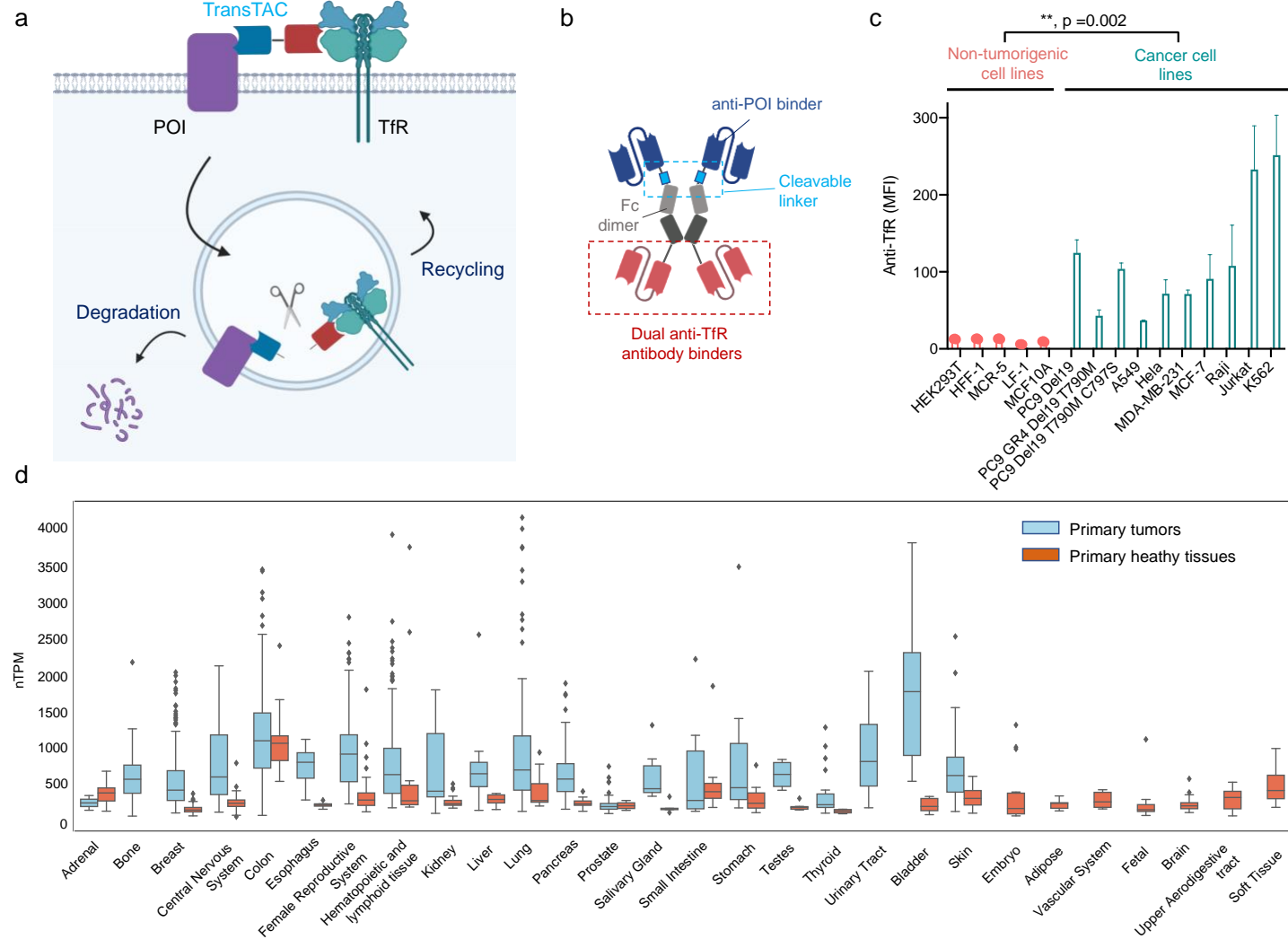
### 69 **TfR1 expression is upregulated in cancer cell lines, primary tumors, and activated T cells**

70 Our rationale for developing the TransTAC technology is that overexpression of TfR1 in malignant tissues  
71 may enable enhanced tumor targeting specificities of the degrader. Thus, we sought to validate cancer-specific  
72 TfR1 overexpression and analyze its tissue distribution. Cell surface TfR1 levels were measured on ten cancer  
73 cell lines and five non-tumorigenic cell lines, including lung, breast, cervical, lymphoma, and leukemia cancers  
74 (**Fig. 1c**). TfR1 overexpression was observed on all cancer cell lines compared to normal cell lines with statistical  
75 significance ( $p = 0.002$ ). Among different cell types, Jurkat and K562 leukemia cell lines exhibited the highest  
76 TfR1 expression, with more than 20-fold greater TfR1 expression compared to normal cells. Similarly, A549  
77 (EGFR wildtype) and PC9 (EGFR mutant) lung cancer cell lines showed 3 to 11-fold greater TfR1 expression  
78 than normal cells.

79 We further showed TfR1 expression is upregulated in primary tumors compared to primary healthy tissues,  
80 by performing a transcriptomics analysis of *TFR1C*, the gene for TfR1 (**Fig. 1d, Extended Data Fig. 1a**)<sup>19</sup>.  
81 Microarray transcriptomics data of *TFR1C* was obtained from the MERA V database<sup>20</sup>. Paired tissue analysis was  
82 performed using a custom python script (**SI Appendix**). *TFR1C* expression is statistically significantly increased  
83 in cancers overall ( $p = 3.98e-89$ ) and in 14 out of 19 specific tissues, including breast, lung, pancreas, liver,

84 bladder, skin, esophagus, thyroid, testes, stomach, salivary gland, kidney, central nerves system (CNS), and  
 85 female reproductive system tumors. Adrenal samples exhibited higher *TFR1C* levels in healthy tissues, but  
 86 without statistical significance. Small intestine, prostate, colon, and hematopoietic and lymphoid samples had  
 87 higher overall expression of *TFR1C* in tumor than normal tissues, but without statistical significance. The lack of  
 88 statistical significance for hematopoietic and lymphoid samples may be due to heterogeneity of various subsets  
 89 of cell types. Among all measured healthy tissues, colon tissues had the highest basal *TFR1C* expression.

90 To investigate whether TfR1 could also be a potential target for immune cell modulation, the DICE dataset  
 91 was analyzed, which contains gene expression profiles of human immune cells isolated from blood samples of  
 92 healthy donors<sup>21</sup>. While most immune cells express a low level of TfR1s, an approximately 6-fold higher TfR1  
 93 expression in activated CD4 and CD8 T cells was observed compared to inactivated T cells, a level comparable  
 94 to the TfR1 levels in some malignant tissues, indicating TfR1 is also a promising target for modulating activated  
 95 T cells (**Extended Data Fig. 1b,c**). Together, our analysis of TfR1 expression in cell lines, primary cancer and  
 96 healthy tissues, and primary immune cells reveal the potential of targeting TfR1 for specific modulation of tumor  
 97 cells and activated T cells. Our transcriptomic analysis provides a detailed comparison of TfR1 expression in  
 98 specific tissues, serving as a roadmap for future selection of disease indications for our technology and beyond.



99  
 100 **Figure 1. Overview of the TransTAC technology and Transferrin Receptor 1 (TfR1) expression analysis.** (a) Schematic of  
 101 TransTACs. TransTAC induces close proximity of TfR and a protein of interest (POI) at the cell surface, leading to co-internalization  
 102 of the complex to the early endosomes, where a cathepsin enzyme cleaves TransTAC and separates the POI from the TfR. The POI then

103 traffics to late endosomes/lysosomes for degradation, while TfR is recycled back to the cell surface. **(b)** Illustration of an example  
104 TransTAC protein. Key designs to make TransTACs efficient degraders include: (1) containing two anti-TfR1 binders for binding and  
105 priming a TfR1 dimer for endocytosis, (2) having a cathepsin-sensitive linker between the anti-POI binder and the Fc for endosomal  
106 cleavage to separate the POI from the recycling TfR1s, and (3) using an antibody binder instead of a native TfR1 ligand to reduce  
107 trafficking to the recycling endosomes. **(c)** Relative cell surface TfR1 expression levels across various non-tumorigenic and cancer cell  
108 lines characterized by flow cytometry. Cancer cell lines express significantly higher levels of TfR1 compared to non-tumorigenic cell  
109 lines. Data are representative of 3 independent experiments. **(d)** Relative *TFR1C* RNA expression levels in primary tumor compared to  
110 normal tissues based on the MERA V database. *TFR1C* expression is significantly higher in most tumors than the corresponding normal  
111 tissues. T-test in **Extended Data Fig. 1a** shows significance for comparing tumors to healthy tissue overall ( $p= 3.98e-89$ ), and for 14  
112 out of 19 of the individual tumor/healthy tissue pairs. Female reproductive tissues are the endometrium, cervix, fallopian tubes,  
113 myometrium, ovary, placenta, and uterus. Central nervous system (CNS) tissues are the basal ganglia, brainstem, cerebral cortex,  
114 hippocampus, spinal cord, and vestibular nuclei superior. Brain tissues are the hypothalamus, pituitary gland, thalamus, ganglia, and  
115 ganglion nodose. Full sample IDs and labels are available in **SI appendix table**. Error bars represent standard deviations. Fig. 1a, b are  
116 created with BioRender.com.

## 117 118 The Rational Design and Optimization of TransTAC Degraders

119 We next set out to design TransTACs. Generally, TransTACs are recombinant proteins consisting of anti-  
120 POI and anti-TfR1 binders to bring the POI and TfR1 in close proximity on the cell surface. However, we  
121 identified three crucial design principles that are important for making TransTACs efficient degraders: (1) *dimeric*  
122 TransTACs are more effective at driving protein internalization than monomeric ones, (2) a *cathepsin-sensitive*  
123 *linker* is necessary for POI separation from TfR1 and lysosomal trafficking, and (3) using an *antibody binder* to  
124 target TfR1, rather than a native transferrin (TF) ligand, can minimize POI trafficking to the recycling endosomes  
125 (REs) and increase degradation efficiency (**Fig. 1b**). Here, we describe how these principles were discovered,  
126 using the anti-CD19 chimeric antigen receptor (CAR)-TransTAC as an example.

127 Our first discovery was that a dimeric TransTAC is more effective than a monomer in internalizing CAR.  
128 Two versions of TransTAC were made: v0.1, a knob-in-hole (KIH) Fc heterobispecific, and v0.2, a homodimeric  
129 Fc fusion (**Fig. 2a**). The TfR1 ligand TF was used for binding TfR1. A stable CD19 ectodomain variant,  
130 CD19NT.1, evolved by yeast display, was used for binding CAR<sup>22</sup>. A CD19NT.1-Fc fusion showed a  
131 homogeneous band in the SDS-PAGE gel, whereas a native CD19 ectodomain-Fc showed aggregations,  
132 indicating that using the engineered binder was necessary (**Extended Data Fig. 2**). CAR-TransTACv0.1 and 0.2,  
133 along with a control lacking the TF ligand, were recombinantly expressed and incubated with Jurkat T lymphocyte  
134 cells expressing a Myc-tagged CAR overnight (**Fig. 2b**). Cell surface CAR levels were measured using an anti-  
135 Myc antibody. Both v0.1 and v0.2 substantially decreased cell surface CAR levels, with a maximal percent  
136 decrease ( $D_{max}$ ) of approximately 60% for v0.1 and 80% for v0.2 (**Fig. 2c**). CAR internalization was dependent  
137 on binding to TfR1, as the control CD19NT.1-Fc did not result in a decrease in cell surface CAR levels.  
138 Intriguingly, a hook effect was observed with v0.1, but not v0.2. This is potentially because avidity could promote  
139 cooperative binding and hence simultaneous engagement of POIs and TfR1s at the cell surface, reducing the hook  
140 effect within a broader concentration range<sup>23</sup>. Overall, the observation of dimeric TransTACs being more effective  
141 is consistent with the notion that TfR1 is a homodimeric receptor and requires binding of two TFs to fully prime  
142 its physiological functions<sup>24</sup>.

143 Interestingly, despite the effective cell surface removal of CAR, TransTACv0.2 did not result in CAR  
144 degradation, as shown by whole-cell lysate western blots (**Fig. 2d, Extended Data Fig. 3a, b**). To understand the  
145 subcellular destination of the internalized CAR, we stably expressed CAR-GFP and mCherry tagged to different  
146 endosomal and lysosomal markers, including Rab5+ or EEA+ for early endosomes (EEs), Rab7+ for late

147 endosomes (LEs), Rab11+ for REs, and Lamp1+ for lysosomes, in a HeLa cell line (**Fig. 2i, j, Extended Data**  
148 **Fig. 4**)<sup>25</sup>. Fluorescence microscopy imaging of v0.2-treated cells showed co-localization of CAR-GFP with Rab11,  
149 indicating that the internalized CAR trafficked to the REs with v0.2 (**Fig. 2i, white arrows**).

150 To promote CAR entry into the degradative pathway and prevent sorting into the recycling pathway with  
151 TfR1, we incorporated a cathepsin-sensitive linker for proteolytic processing in the EEs<sup>26</sup>. We reasoned that to  
152 prevent CAR from being sorted into the recycling pathway and instead promote its entry into the degradative  
153 pathway, it would be necessary for CAR to disengage from TfR1 in the EEs (**Fig. 2e,f**). A cathepsin-sensitive  
154 sequence was inserted in TransTACs, either between Fc and TF (v0.3), or between CD19NT.1 and Fc (v0.4) (**Fig.**  
155 **2a, Extended Data Fig. 3a**). Western blot analysis of CAR-Jurkat cells treated with v0.4 showed approximately  
156 40-50% degradation of CAR (**Extended Data Fig. 3c**). Furthermore, HeLa cells expressing CAR-GFP treated  
157 with v0.4 showed a substantial reduction in GFP fluorescence (**Fig. 2i, j, Extended Data Fig. 4a-c**), showing the  
158 new linker design enabled protein degradation.

159 To determine whether trafficking to LEs and lysosomes was enhanced, we collected fluorescence images  
160 for Pearson correlation analysis of GFP and mCherry. A significant increase was observed in CAR-GFP/Rab7  
161 and Lamp1 co-localization, markers for LEs and lysosomes, compared to co-localization with Rab11, validating  
162 our hypothesis that endosomal sorting to the degradative pathway was enhanced with the linker variation (**Fig. 2i,**  
163 **Extended Data Fig. 4d, 5**). Interestingly, the degradation efficiency was substantially lower with v0.3 (**Extended**  
164 **Data Fig. 3c**). This is possibly because CD19NT.1 remains linked to the Fc after cleavage of TransTACv0.3, and  
165 Fc can subsequently mediate protein recycling via the FcRn pathway<sup>27</sup>.

166 We further screened a panel of linkers to identify optimal protease substrates in EEs<sup>28</sup>. Fourteen linkers  
167 containing single or combined cathepsin cleavage motifs were incorporated into the CAR-TransTAC and  
168 characterized using western assays (**Extended Data Fig. 3d,e**)<sup>29</sup>. Two of the best linkers from this panel were  
169 selected to develop new TransTACs.

170 Lastly, we substituted TF with an anti-TfR1 single-chain Fv (scFv) identified from phage display. Our  
171 rationale was that TF may contain specific structural or signaling elements that promote trafficking of internalized  
172 proteins to the REs. Therefore, using a synthetic antibody may reduce trafficking of the internalized complex to  
173 the REs, resulting in an increased percentage of POIs that stay in the EE compartments for proteolytic processing  
174 and trafficking to the degradative pathway (**Fig. 2g, h**). Two new TransTACs were generated: v0.5 containing  
175 the anti-TfR1 scFv binder but no cleavable linker, and v1.0 containing both the anti-TfR1 scFv and the cleavable  
176 linker (**Fig. 2a**). Remarkably, cells treated with v0.5 showed strong colocalization of CAR-GFP with EE markers  
177 Rab5 and EEA, but not RE marker Rab11 (**Fig. 2i, j, Extended Data Fig. 4a**). Pearson colocalization coefficients  
178 of the corresponding markers were statistically different from cells treated with TransTACv0.2, which contains  
179 the TF ligands (**Fig. 2k, Extended Data Fig. 4d**). Additionally, protein degradation efficiency was substantially  
180 increased. With v1.0, over 80% CAR degradation was observed in the Western, and nearly no CAR-GFP signals  
181 were observed in fluorescence images (**Fig. 2d, i, j, Extended Data Fig. 4a-c**). Additionally, the anti-TfR1 scFv  
182 substitution also increased the yield of the protein by approximately seven-fold, making the expression level of  
183 TransTACs similar to that of conventional antibodies.

184 Taken together, our rational protein engineering efforts have successfully rewired the intracellular  
185 trafficking of the target protein in the endosomal-lysosomal pathway, resulting in a novel protein degrader design,  
186 TransTACv1.0, that leads to >80% CAR degradation. Notably, several earlier versions of CAR-TransTACs have

187 the ability to effectively eliminate CAR from the cell surface through an endosomal trapping mechanism, offering  
188 versatile possibilities of membrane protein regulation (**Fig. 2a**).

189 CAR-T cell therapy has demonstrated significant potential in treating hematologic malignancies. However,  
190 its broad application is limited by the risk of potentially fatal side effects, such as cytokine release syndrome  
191 (CRS), caused by the overactivation of CAR-T cells<sup>30,31</sup>. To this end, CAR-TransTACs can potentially serve as a  
192 modular protein OFF switch to fine tune CAR-T cell activity and to manage its associated toxicities (**Extended**  
193 **Data Figure 6a**). As a proof of concept, we showed that CAR-TransTACv0.4 can effectively inhibit human  
194 primary CAR-T cell IFN- $\gamma$  secretion, giving an impressively low IC<sub>50</sub> of 0.4 nM (**Extended Data Figure 6b, c**).  
195 Additionally, it reversibly regulated CAR-T cell-mediated tumor killing activities (**Extended Data Figure 6b, d,**  
196 **e**). To the best of our knowledge, CAR-TransTAC is the first recombinant protein-based OFF-switch for CAR-T  
197 cell regulation that does not need additional modifications to the CAR-T cells. Unlike splitCAR- or other circuit  
198 rewiring-based methods<sup>31</sup>, CAR-TransTACs do not require genetic engineering and are, therefore, readily  
199 adaptable to a variety of CAR-T cell therapies, both approved and in development.

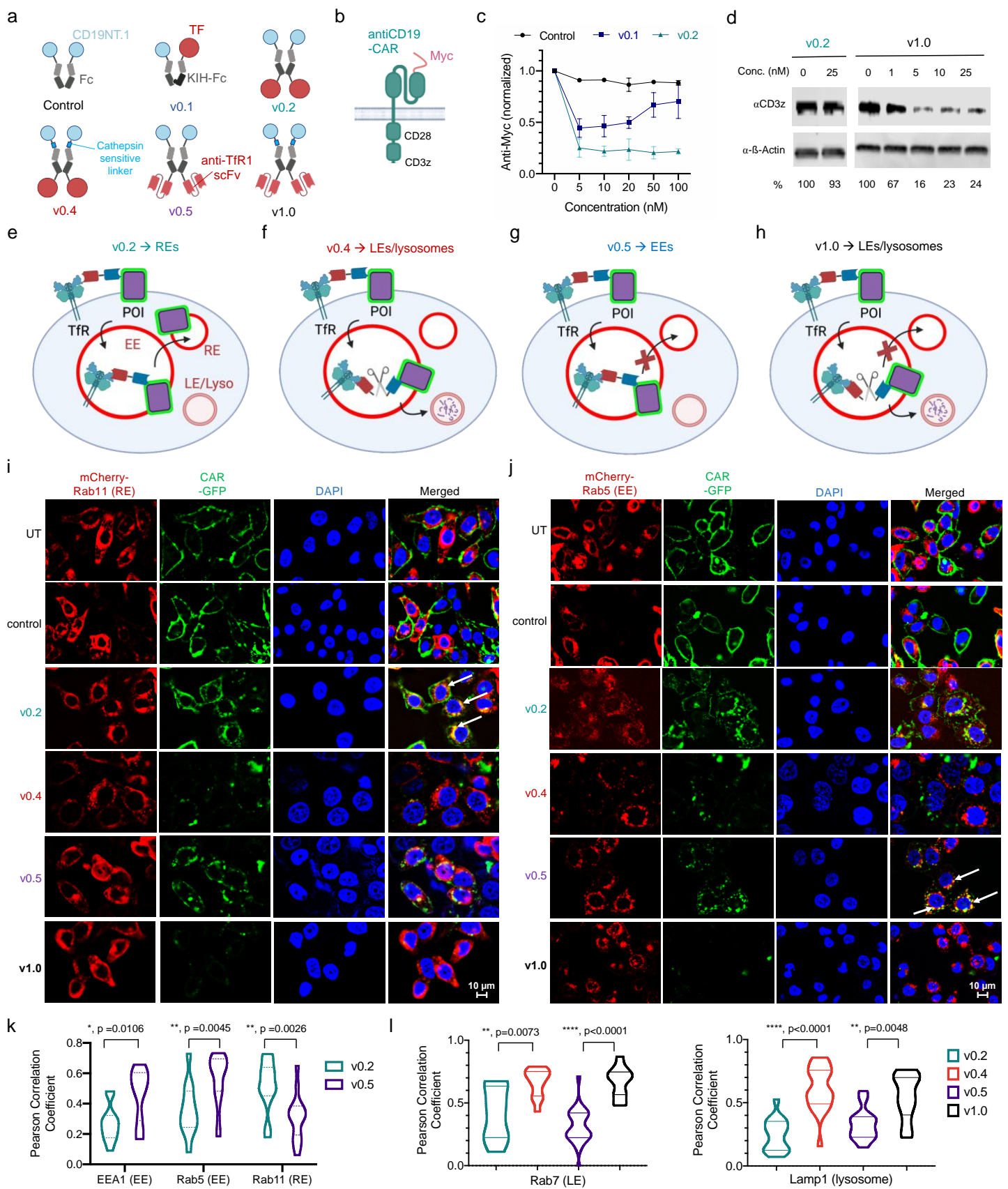


**Figure 2. TransTAC degrader engineering.** (a) Schematic of CAR-TransTACs and control. TransTACv0.1 consists of a single CD19NT.1 domain, a single TF, and a knob-in-hole (KIH) Fc, v0.2 consists of two CD19NT.1s, two TFs, and a homodimeric Fc that connects the binders, v0.4 contains a cathepsin-sensitive linker between CD19NT.1 and Fc, v0.5 contains an anti-TfR1 scFv for TfR1 binding, v1.0 contains both the anti-TfR1 scFv and the cathepsin-sensitive linker. (b) Schematic of a Myc-tagged anti-CD19 CAR

205 receptor. **(c)** Flow cytometry measurements of cell surface CAR expression levels in CAR-Jurkats treated with TransTACv0.1, v0.2,  
206 and control. TransTACv0.2 results in higher CAR clearance from cell surface than v0.1 and no hook effect. Data are representative of  
207 2 independent experiments. Error bars represent standard deviations. **(d)** Characterization of whole-cell CAR levels by Western blot in  
208 CAR-Jurkats treated with TransTACs. TransTACv1.0 degrades approximately 80% of CAR; v0.2 did not result in significant CAR  
209 degradation. **(e-h)** Schematics showing different TransTACs alter intracellular trafficking of the POI. Cleavage of the cathepsin-sensitive  
210 linker in v0.4 and v1.0 leads to separation of POI from TfR1, hence enhancing LE/lysosomal trafficking of the POI and degradation;  
211 the anti-TfR1 scFv in v0.5 and v1.0 reduces trafficking of the complex to the REs, hence increasing the proportion of POI in EEs and  
212 subsequent proteolytic processing, when a cleavable linker is present. **(i, j)** Representative fluorescence images of HeLa cells co-  
213 expressing CAR-GFP (green) and endosomal/lysosomal markers-mCherry (red) treated with various TransTAC molecules. Cell nucleus  
214 is stained with Hoechst (blue). Untreated (UT) or control-treated cells had CAR-GFP localized at the cell membrane. v0.5 and v1.0 led  
215 to efficient degradation of CAR-GFP, manifested by the significantly lower GFP signals. v0.2-treated cells predominantly trafficked  
216 CAR to the REs, showing co-localization of CAR-GFP with mCherry-Rab11 (white arrows). v0.5-treated cells trafficked CAR to the  
217 EEs, showing co-localization of CAR-GFP with mCherry-Rab5 (white arrows). **(k)** Pearson correlation analysis of CAR-GFP  
218 colocalization with the Rab5 (EE), EEA1 (EE), and Rab11 (RE) markers. T-tests show Rab5, EEA1, Rab11 colocalization with CAR  
219 are statistically different for cells treated with v0.2 vs. v0.5. **(l)** Pearson correlation analysis of CAR-GFP colocalization with the Rab7  
220 (LE) and Lamp1 (lysosome) markers. T-tests show Rab7 and Lamp1 colocalization with CAR are statistically significant for v0.2 vs.  
221 v0.4, and v0.5 vs. v1.0. For k and l, the number of cells used for each analysis are as follows: For v0.2, N=12, N=12, and N=13 for the  
222 EEA1, Rab5 and Rab11 markers, respectively. For v0.5, N=10, N=22, and N=15 for the EEA1, Rab5 and Rab11 markers respectively.  
223 For v0.2, v0.4, v0.5, and v1.0 with the Lamp1 marker N=16, N=21, N=13, and N=13, respectively. Fig. 2a, b, e-h are created with  
224 BioRender.com.

## 225 Expansion of TransTAC-addressable targets

226 We next established the generalizability of TransTAC degraders (**Fig. 3a**). We aimed to include targets  
227 that have diverse structures and functions present on different cell types, such as native vs. synthetic, single-pass  
228 vs. multi-pass transmembrane, and cancer vs. immune cell targets.

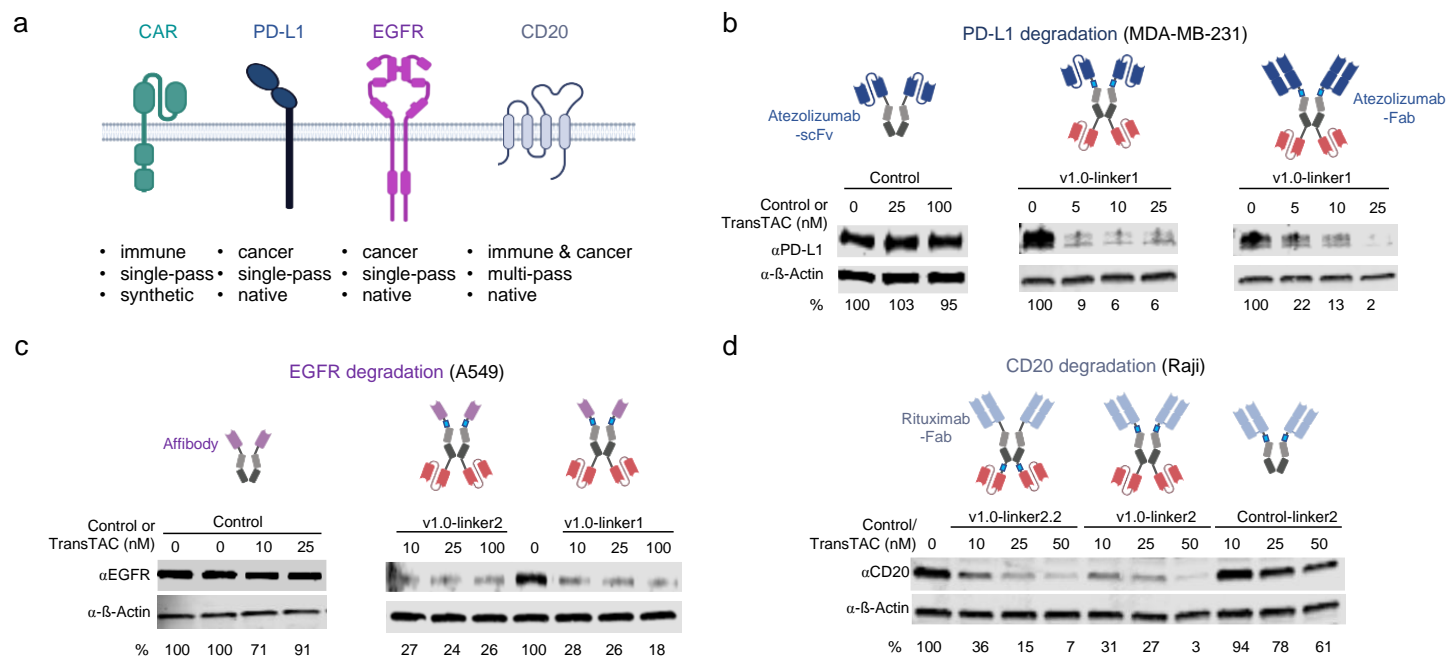
229 Our first target is programmed death-ligand 1 (PD-L1), an immune checkpoint receptor ligand,  
230 downregulation of which can enhance anti-tumor T cell activity<sup>32</sup>. Despite having improved clinical outcomes  
231 across tumors, many patients still do not benefit from monoclonal antibodies targeting the PD-1/PD-L1 axis,  
232 making new mechanisms for targeting PD-L1 highly desirable. A PD-L1-TransTAC was created using a fragment  
233 antigen binding (Fab) or single-chain variable fragment (scFv) of atezolizumab as the PD-L1 binding domain  
234 (**Fig. 3b**)<sup>33</sup>. Up to 98% PD-L1 degradation was observed in MDA-MB-231 breast cancer cells treated with PD-  
235 L1-TransTACs, while control groups lacking the anti-TfR1 scFv binder or containing TransTACv0.2 and v0.4  
236 with a TF ligand showed no or little PD-L1 degradation (**Fig. 3b, Extended Data Fig. 7a**).

237 Next, we aimed to target EGFR, a receptor tyrosine kinase that plays a critical role in the development  
238 and progression of various types of cancers such as lung and brain<sup>34</sup>. An EGFR-TransTAC was created with an  
239 affibody as the EGFR binding domain (**Fig. 3c**)<sup>35</sup>. A549 lung carcinoma cells treated with EGFR-TransTACv1.0s  
240 showed up to 80-90% reduction of EGFR, whereas control groups exhibited little to no degradation (**Fig. 3c, Extended Data Fig. 7b**). Different linkers in v1.0 resulted in varying degrees of EGFR degradation, while v0.2  
241 had no effect (**Extended Data Fig. 7b**). These results were consistent with the observations with the CAR-  
242 TransTAC variants, validating the importance of those modifications made to improve TransTAC efficiency.

243 Cluster of differentiate 20 (CD20) is a B cell-specific surface marker with four transmembrane domains  
244 and an unknown function<sup>36</sup>. Knocking down cell surface CD20s with a degrader could be valuable for functional  
245 studies of CD20. Using a scFv and a Fab format of rituximab, the first clinically approved antibody directed  
246 against CD20 in the setting of non-Hodgkin lymphoma, we created a CD20-TransTAC (**Fig. 3d**)<sup>37</sup>. Treatment of

249 Raji cells, a human B lymphoblastoid cell line, with the CD20-TransTAC resulted in up to 97% reduction of  
250 CD20, while control groups led to no or significantly less degradation (**Fig. 3d, Extended Data Fig. 7c**).

251 Together, the successful generation of degraders against all four targets demonstrates the modularity and  
252 generality of the TransTAC design. Importantly, high potencies were observed for all four targets, highlighting  
253 the efficiency of targeted degradation using TransTACs.



254  
255 **Figure 3. Developing TransTACs degraders for various proteins.** (a) Schematic of membrane proteins targeted by TransTACs in  
256 the present study. These targets are either synthetic, or native, single- or multi-pass proteins expressed on the cancer or immune cell  
257 surface. (b) PD-L1 degradation by TransTACs in MDA-MB-231 breast cancer cells analyzed by Western blot. A scFv or Fab format of  
258 atezolizumab is used as the PD-L1 binding moiety. (c) EGFR degradation by TransTAC in A549 lung carcinoma cells. An affibody is  
259 used as the EGFR binding moiety. (d) CD20 degradation by TransTAC. A Fab format of rituximab is used as the CD20 binding moiety.  
260 Fig. 3a and illustrations of TransTACs in 3b-d are created with BioRender.com.

## 261 262 Kinetics, structure-activity relationship, mechanism, and *in vivo* characterization of TransTACs

263 We then studied the kinetics of TransTAC-mediated protein internalization. A time-course measurement  
264 of cell surface CAR levels in response to TransTACs was performed (**Fig. 4a**). A rapid elimination of CAR from  
265 the cell surface was observed, with only 17% remaining after 10 minutes and 13% after 20 minutes of treatment  
266 with TransTACv1.0. Furthermore, this response was long-lasting, with 10% of CAR observed at the cell surface  
267 after 3 hours with v1.0. This fast and sustained protein downregulation highlights TransTACs as a promising  
268 research tool for knocking down cell surface proteins as an alternative to genetic methods.

269 To further understand how the number of binders and geometry of TransTACs influence its behavior, we  
270 generated and tested four CAR-TransTACv0.5 variants, v0.6-v0.9, each containing one or two copies of  
271 CD19NT.1 or anti-TfR1 scFv (**Fig. 4b**). Our findings revealed that having two anti-TfR1 binders was more critical  
272 than having two CD19NT.1s in enhancing CAR internalization (v0.6 vs. v0.7, **Fig. 4c**). This highlights the  
273 importance of dual binding to a dimeric TfR1, rather than having two anti-POI binders, in creating a potent  
274 TransTAC. It also indicated that TransTAC-mediated CAR internalization was not the result of CAR crosslinking.  
275 Additionally, we observed significant differences in the internalization efficiency for molecules with different

276 geometries, indicating that the geometry of the tertiary complex structure plays a role in influencing TransTAC  
277 efficiency (v0.8 vs. v0.9, **Fig. 4c**). Furthermore, we generated an Fc-anti-TfR1 scFv molecule as a competitor for  
278 TfR1 binding and observed a dose-dependent decrease of CAR internalization in the presence of the competitor  
279 in solution with TransTACv0.5 treatment (**Fig. 4d**). This observation further validates that TransTACs function  
280 through a TfR1-dependent mechanism. These structure-activity relationship analyses offer valuable insights to  
281 guide future TransTAC designs.

282 We next investigated the cellular mechanism underlying TransTAC-mediated protein degradation. Two  
283 primary pathways involved in the degradation of cellular proteins were tested: the lysosomal pathway and the  
284 proteasome pathway<sup>38</sup>. A549 cells were treated either with bafilomycin, a vacuolar proton pump inhibitor that  
285 inhibits lysosomal acidification<sup>39</sup>, or MG132, a proteasomal inhibitor<sup>40</sup>. We observed 1  $\mu$ M bafilomycin  
286 prevented TransTAC-mediated EGFR degradation, whereas 1  $\mu$ M MG132 had a much less significant effect (**Fig.**  
287 **4e**). These results show that intact lysosomal function was essential for TransTAC-mediated protein degradation.

288 To determine whether TfR1 level remains consistent or reduced with TransTAC treatment, we  
289 characterized whole-cell TfR1 expression using Western blotting assay with a PD-L1-TransTAC in the MDA-  
290 MB-231 cell line. No change in TfR1 level was observed, which is in clear contrast to the loss of PD-L1 in the  
291 same assay (**Fig. 4f**). This result validates our hypothesis that the POI was separated from TfR1 before being  
292 routed to degradation, while TfR1 is recycled.

293 Lastly, we asked whether TransTACs would be well tolerated and have similar antibody clearance to IgGs  
294 *in vivo*. We intraperitoneally injected 5 or 7 mg/kg (body weight) CD20-TransTAC or 5 mg/kg IgG control into  
295 nude mice (**Fig. 4g**). No significant weight changes were observed with either the TransTACs or the control (**Fig.**  
296 **4h**). Western blotting analysis of plasma antibody levels revealed that the TransTAC remained in plasma up to  
297 10 days after injection, which is comparable to the reported half-life of IgGs in mice (**Fig. 4i, Extended Data Fig.**  
298 **8**)<sup>41</sup>. It was known that the anti-TfR1 antibody we used is cross-reactive with mouse TfR1. Together, these results  
299 demonstrate that TransTACs are well-tolerated, have favorable pharmacokinetics, and are not being rapidly  
300 cleared despite cross-reactivity with mouse cells.

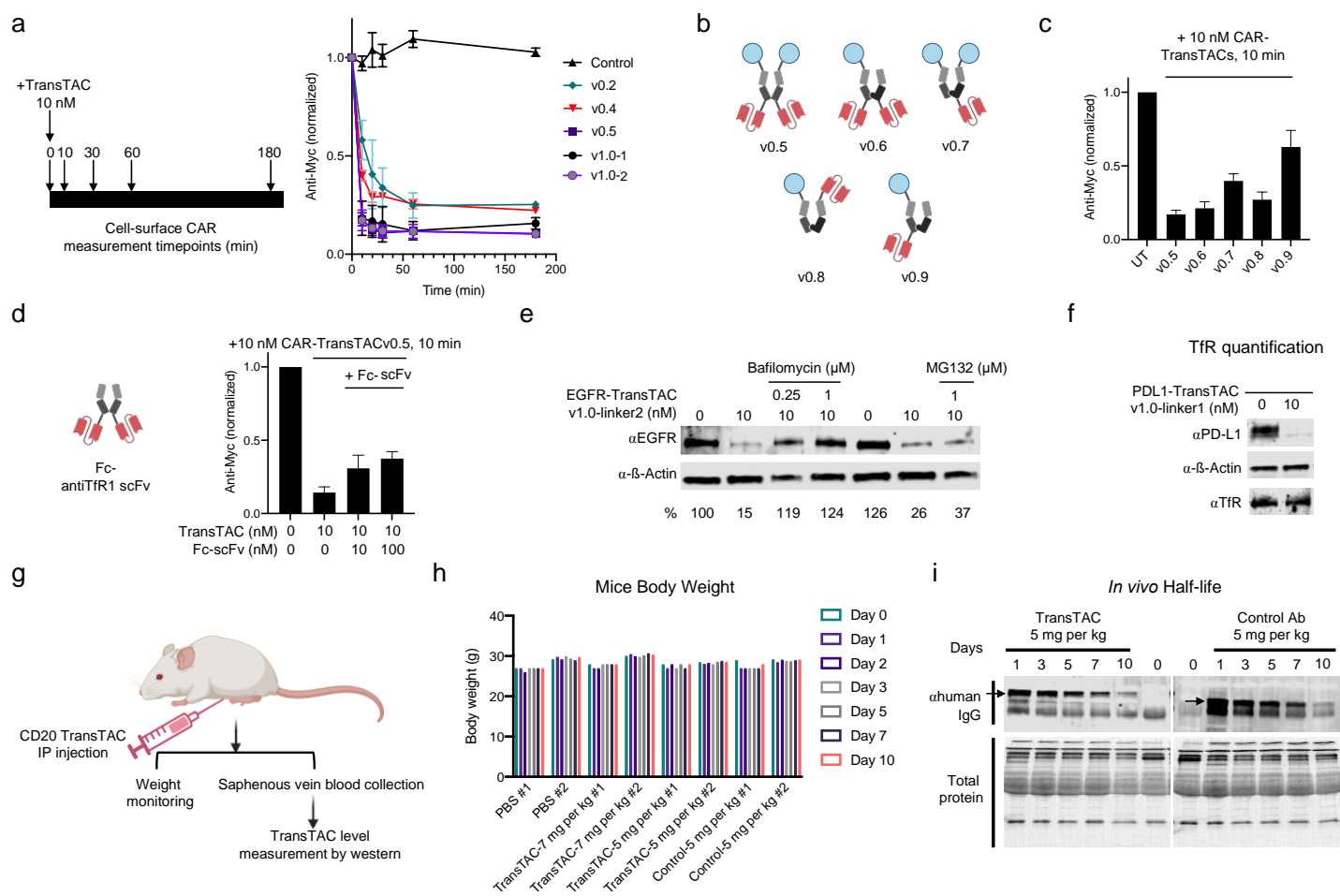


**Figure 4. Structure-activity relationship of TransTACs, mechanisms, and *in vivo* characterizations.** (a) Time-course measurement of cell surface CAR levels in CAR-Jurkats treated with TransTACs, revealing the fast kinetics of TransTAC-mediated CAR internalization. (b) Schematics of CAR-TransTAC variants consisting of one or two copies of anti-POI and anti-TfR1 binders in different protein geometries. (c) Cell surface CAR level measurements in CAR-Jurkats treated with CAR-TransTAC variants outlined in (b). The results highlight the impacts of having two vs. one TfR1 binders (v0.5 vs v0.7) and geometry (v0.8 vs. v0.9) in modulating protein internalization. Data are representative of 3 independent measurements. (d) Competition assay with a Fc-anti-TfR1 scFv fusion protein. Concentration-dependent reduction of CAR internalization is observed with Fc-anti-TfR1 scFv, proving internalization is mediated through TfR1. Data are representative of 3 independent measurements. (e) Study of underlying degradation pathways with TransTACs. Intact lysosomal function is critical for degradation, as degradation is fully inhibited by bafilomycin in A549 cells treated with EGFR-TransTACs. (f) Whole-cell TfR1 level measurement with TransTAC treatment. TfR1 level stays consistent while PD-L1 is degraded in MDA-MB-231 cells treated with PD-L1 TransTAC. (g) Schematic of mouse experiments to assess TransTAC safety and serum half-life via IP injection. (h) Weight monitoring of mice over time after TransTAC or control IgG injection. Results reveal no observable effects on mouse weight over time, showing molecules are well tolerated. N=2 per treatment group. (i) Western blots of plasma levels of CD20-TransTAC and control IgG over time, with quantification of data in **Extended Data Fig. 8**. Results reveal TransTAC remained in plasma up to 10 d after injection. N=2 per treatment group. Illustrations in Fig. 4b, d, g are created with BioRender.com.

## **Discussion:**

Membrane proteins, accounting for approximately one-third of all human proteins, play pivotal roles in numerous cellular functions<sup>3</sup>. The ability to precisely down-regulate these proteins, ideally with temporal resolution, is crucial for studying and manipulating their physiological and disease-related functions. In this study, we introduced TransTAC, a novel molecular archetype for degrading membrane proteins. TransTACs achieved impressive degradation efficacies for various structurally and functionally diverse proteins, resulting in >80%

324 maximal degradation across different cancer cell lines and targets. Notably, we demonstrated the first examples  
325 of using a bispecific antibody to degrade a multi-pass membrane protein, CD20, and a synthetic receptor, CAR,  
326 extending beyond targets previously explored in other studies. TransTACs are fully recombinant, easily produced,  
327 and compatible with various protein binding moieties, including Fab, scFv, affibody or protein ectodomains.  
328 These findings underscore the modularity of TransTAC designs.

329 A distinguishable advantage of TransTAC is its potential tumor specificity. Our analysis of TfR1  
330 expression supports previous findings that TfR1 is significantly upregulated in cancer cells. Consequently, our  
331 developed TransTACs may enable selective targeting of cancer cells while minimizing toxicity to normal cells,  
332 addressing the off-target effects commonly associated with traditional cancer treatments.

333 TransTAC is the first protein degrader design to hijack a naturally recycling pathway, rather than a  
334 lysosome-shuttling ligand, for targeted protein degradation. Achieving this required a combination of protein  
335 engineering approaches, such as utilizing protein dimers, incorporating a cleavable linker, and employing an  
336 antibody instead of a natural ligand for effector binding. These engineering strategies proved to be remarkably  
337 effective, and we believe they may be generalizable to other cell surface effectors, broadening the potential scope  
338 of cell surface effectors viable for protein degradation.

339 The TransTAC technology is versatile and adaptable. By employing specific variants of the molecules,  
340 researchers can induce either endosomal trapping or lysosomal degradation of targets, allowing for customizable  
341 and modular manipulation of membrane proteins. Additionally, a distinguishing feature of TransTACs is their  
342 ability to rapidly control protein internalization, on a timescale of minutes in the context of CAR. This  
343 characteristic offers immense potential for fundamental research focused on understanding the temporal  
344 regulation of membrane protein functions and associated cell signaling pathways. In summary, TransTAC  
345 represents a novel protein degrader design for targeting cell surface proteins. Its tumor and immune cell specificity,  
346 genetic tractability, and rapid internalization kinetics promise to have a substantial impact on both fundamental  
347 research and therapeutic applications.

## 348

## 349 References:

- 350 1 Békes, M., Langley, D. R. & Crews, C. M. PROTAC targeted protein degraders: the past is prologue. *Nat Rev Drug Discov* **21**, 181-200 (2022). <https://doi.org/10.1038/s41573-021-00371-6>
- 351 2 VanDyke, D., Taylor, J. D., Kaeo, K. J., Hunt, J. & Spangler, J. B. Biologics-based degraders - an  
352 expanding toolkit for targeted-protein degradation. *Curr Opin Biotechnol* **78**, 102807 (2022).  
<https://doi.org/10.1016/j.copbio.2022.102807>
- 353 3 Uhlen, M. *et al.* Proteomics. Tissue-based map of the human proteome. *Science* **347**, 1260419 (2015).  
<https://doi.org/10.1126/science.1260419>
- 354 4 Cotton, A. D., Nguyen, D. P., Gramespacher, J. A., Seiple, I. B. & Wells, J. A. Development of Antibody-  
355 Based PROTACs for the Degradation of the Cell-Surface Immune Checkpoint Protein PD-L1. *J Am Chem Soc* **143**, 593-598 (2021). <https://doi.org/10.1021/jacs.0c10008>
- 356 5 Marei, H. *et al.* Antibody targeting of E3 ubiquitin ligases for receptor degradation. *Nature* (2022).  
<https://doi.org/10.1038/s41586-022-05235-6>
- 357 6 Ahn, G. *et al.* LYTACs that engage the asialoglycoprotein receptor for targeted protein degradation. *Nat Chem Biol* **17**, 937-946 (2021). <https://doi.org/10.1038/s41589-021-00770-1>
- 358 7 Banik, S. M. *et al.* Lysosome-targeting chimaeras for degradation of extracellular proteins. *Nature* **584**,  
359 291-297 (2020). <https://doi.org/10.1038/s41586-020-2545-9>
- 360 8 Pance, K. *et al.* Modular cytokine receptor-targeting chimeras for targeted degradation of cell surface and  
361 extracellular proteins. *Nat Biotechnol* (2022). <https://doi.org/10.1038/s41587-022-01456-2>

368 9 Zhou, Y., Teng, P., Montgomery, N. T., Li, X. & Tang, W. Development of Triantennary N-  
369 Acetylgalactosamine Conjugates as Degraders for Extracellular Proteins. *ACS Cent Sci* **7**, 499-506 (2021).  
370 <https://doi.org/10.1021/acscentsci.1c00146>

371 10 Daniels, T. R., Delgado, T., Rodriguez, J. A., Helguera, G. & Penichet, M. L. The transferrin receptor part  
372 I: Biology and targeting with cytotoxic antibodies for the treatment of cancer. *Clin Immunol* **121**, 144-158  
373 (2006). <https://doi.org/10.1016/j.clim.2006.06.010>

374 11 Kawabata, H. Transferrin and transferrin receptors update. *Free Radic Biol Med* **133**, 46-54 (2019).  
375 <https://doi.org/10.1016/j.freeradbiomed.2018.06.037>

376 12 Candelaria, P. V., Leoh, L. S., Penichet, M. L. & Daniels-Wells, T. R. Antibodies Targeting the  
377 Transferrin Receptor 1 (TfR1) as Direct Anti-cancer Agents. *Front Immunol* **12**, 607692 (2021).  
378 <https://doi.org/10.3389/fimmu.2021.607692>

379 13 Shen, Y. *et al.* Transferrin receptor 1 in cancer: a new sight for cancer therapy. *Am J Cancer Res* **8**, 916-  
380 931 (2018).

381 14 Daniels-Wells, T. R. & Penichet, M. L. Transferrin receptor 1: a target for antibody-mediated cancer  
382 therapy. *Immunotherapy* **8**, 991-994 (2016). <https://doi.org/10.2217/imt-2016-0050>

383 15 Hogemann-Savellano, D. *et al.* The transferrin receptor: a potential molecular imaging marker for human  
384 cancer. *Neoplasia* **5**, 495-506 (2003). [https://doi.org/10.1016/s1476-5586\(03\)80034-9](https://doi.org/10.1016/s1476-5586(03)80034-9)

385 16 Daniels, T. R. *et al.* The transferrin receptor and the targeted delivery of therapeutic agents against cancer.  
386 *Biochim Biophys Acta* **1820**, 291-317 (2012). <https://doi.org/10.1016/j.bbagen.2011.07.016>

387 17 Iacopetta, B. J. & Morgan, E. H. The kinetics of transferrin endocytosis and iron uptake from transferrin  
388 in rabbit reticulocytes. *J Biol Chem* **258**, 9108-9115 (1983).

389 18 Mayle, K. M., Le, A. M. & Kamei, D. T. The intracellular trafficking pathway of transferrin. *Biochim  
390 Biophys Acta* **1820**, 264-281 (2012). <https://doi.org/10.1016/j.bbagen.2011.09.009>

391 19 Kleven, M. D., Jue, S. & Enns, C. A. Transferrin Receptors TfR1 and TfR2 Bind Transferrin through  
392 Differing Mechanisms. *Biochemistry* **57**, 1552-1559 (2018).  
393 <https://doi.org/10.1021/acs.biochem.8b00006>

394 20 Shaul, Y. D. *et al.* MERAVis a tool for comparing gene expression across human tissues and cell types.  
395 *Nucleic Acids Res* **44**, D560-566 (2016). <https://doi.org/10.1093/nar/gkv1337>

396 21 Schmiedel, B. J. *et al.* Impact of Genetic Polymorphisms on Human Immune Cell Gene Expression. *Cell*  
397 **175**, 1701-1715 e1716 (2018). <https://doi.org/10.1016/j.cell.2018.10.022>

398 22 Klesmith, J. R. *et al.* Retargeting CD19 Chimeric Antigen Receptor T Cells via Engineered CD19-Fusion  
399 Proteins. *Mol Pharm* **16**, 3544-3558 (2019). <https://doi.org/10.1021/acs.molpharmaceut.9b00418>

400 23 Cecchini, C., Pannilunghi, S., Tardy, S. & Scapozza, L. From Conception to Development: Investigating  
401 PROTACs Features for Improved Cell Permeability and Successful Protein Degradation. *Front Chem* **9**,  
402 672267 (2021). <https://doi.org/10.3389/fchem.2021.672267>

403 24 Eckenroth, B. E., Steere, A. N., Chasteen, N. D., Everse, S. J. & Mason, A. B. How the binding of human  
404 transferrin primes the transferrin receptor potentiating iron release at endosomal pH. *Proc Natl Acad Sci  
405 U S A* **108**, 13089-13094 (2011). <https://doi.org/10.1073/pnas.1105786108>

406 25 Wang, D. *et al.* Capping protein regulates endosomal trafficking by controlling F-actin density around  
407 endocytic vesicles and recruiting RAB5 effectors. *eLife* **10** (2021). <https://doi.org/10.7554/eLife.65910>

408 26 Yadati, T., Houben, T., Bitorina, A. & Shiri-Sverdlov, R. The Ins and Outs of Cathepsins: Physiological  
409 Function and Role in Disease Management. *Cells* **9** (2020). <https://doi.org/10.3390/cells9071679>

410 27 Pyzik, M. *et al.* The Neonatal Fc Receptor (FcRn): A Misnomer? *Front Immunol* **10**, 1540 (2019).  
411 <https://doi.org/10.3389/fimmu.2019.01540>

412 28 Pillay, C. S., Elliott, E. & Dennison, C. Endolysosomal proteolysis and its regulation. *Biochem J* **363**, 417-  
413 429 (2002). <https://doi.org/10.1042/0264-6021:3630417>

414 29 Poreba, M. Protease-activated prodrugs: strategies, challenges, and future directions. *FEBS J* **287**, 1936-  
415 1969 (2020). <https://doi.org/10.1111/febs.15227>

416 30 Santomasso, B., Bachier, C., Westin, J., Rezvani, K. & Shpall, E. J. The Other Side of CAR T-Cell  
417 Therapy: Cytokine Release Syndrome, Neurologic Toxicity, and Financial Burden. *Am Soc Clin Oncol  
418 Educ Book* **39**, 433-444 (2019). [https://doi.org/10.1200/EDBK\\_238691](https://doi.org/10.1200/EDBK_238691)

419 31 Brandt, L. J. B., Barnkob, M. B., Michaels, Y. S., Heiselberg, J. & Barington, T. Emerging Approaches  
420 for Regulation and Control of CAR T Cells: A Mini Review. *Front Immunol* **11**, 326 (2020).  
<https://doi.org/10.3389/fimmu.2020.00326>

421 32 Doroshow, D. B. *et al.* PD-L1 as a biomarker of response to immune-checkpoint inhibitors. *Nat Rev Clin  
423 Oncol* **18**, 345-362 (2021). <https://doi.org/10.1038/s41571-021-00473-5>

422 33 Herbst, R. S. *et al.* Atezolizumab for First-Line Treatment of PD-L1-Selected Patients with NSCLC. *N  
425 Engl J Med* **383**, 1328-1339 (2020). <https://doi.org/10.1056/NEJMoa1917346>

426 34 Sabbah, D. A., Hajjo, R. & Sweidan, K. Review on Epidermal Growth Factor Receptor (EGFR) Structure,  
427 Signaling Pathways, Interactions, and Recent Updates of EGFR Inhibitors. *Curr Top Med Chem* **20**, 815-  
428 834 (2020). <https://doi.org/10.2174/1568026620666200303123102>

429 35 Friedman, M. *et al.* Directed evolution to low nanomolar affinity of a tumor-targeting epidermal growth  
430 factor receptor-binding affibody molecule. *J Mol Biol* **376**, 1388-1402 (2008).  
<https://doi.org/10.1016/j.jmb.2007.12.060>

431 36 Pavlasova, G. & Mraz, M. The regulation and function of CD20: an "enigma" of B-cell biology and  
432 targeted therapy. *Haematologica* **105**, 1494-1506 (2020). <https://doi.org/10.3324/haematol.2019.243543>

433 37 Pierpont, T. M., Limper, C. B. & Richards, K. L. Past, Present, and Future of Rituximab-The World's First  
434 Oncology Monoclonal Antibody Therapy. *Front Oncol* **8**, 163 (2018).  
<https://doi.org/10.3389/fonc.2018.00163>

435 38 Zhao, L., Zhao, J., Zhong, K., Tong, A. & Jia, D. Targeted protein degradation: mechanisms, strategies  
436 and application. *Signal Transduct Target Ther* **7**, 113 (2022). <https://doi.org/10.1038/s41392-022-00966-4>

437 39 Wang, R. *et al.* Molecular basis of V-ATPase inhibition by bafilomycin A1. *Nat Commun* **12**, 1782 (2021).  
<https://doi.org/10.1038/s41467-021-22111-5>

438 40 Kisseelev, A. F. & Goldberg, A. L. Proteasome inhibitors: from research tools to drug candidates. *Chem  
439 Biol* **8**, 739-758 (2001). [https://doi.org/10.1016/s1074-5521\(01\)00056-4](https://doi.org/10.1016/s1074-5521(01)00056-4)

440 41 Vieira, P. & Rajewsky, K. The half-lives of serum immunoglobulins in adult mice. *Eur J Immunol* **18**,  
441 313-316 (1988). <https://doi.org/10.1002/eji.1830180221>

442 446